

**Application of susceptibility weighted imaging (SWI) for evaluation of draining
veins of arteriovenous malformation: Utility of magnitude images.**

Toshiteru Miyasaka¹, Toshiaki Taoka¹, Hiroyuki Nakagawa¹,
Takeshi Wada¹, Katsutoshi Takayama¹, Kaoru Myochin¹,
Masahiko Sakamoto¹, Tomoko Ochi¹, Kimihiko Kichikawa¹

¹Department of Radiology, Nara Medical University

Corresponding author

Toshiteru Miyasaka¹ M.D.

Department of Radiology, Nara Medical University,

840 Shijo-cho, Kashihara, Nara, 634-8522, Japan

Tel: +81-744-29-8900

Fax: +81-744-24-1988

Email: michy@altgo.net

Abstract

Background and Purpose: The current study evaluated the signal characteristics of SWI of AVM, especially for draining veins. For this purpose, we identified the draining veins of the AVM on angiography and evaluated the signal on magnitude image for SWI (SWI-mag) and minimum-intensity projection image (SWI-minIP).

Materials and Methods: Subjects were 14 patients with angiographically proven AVM. SWI-mag, SWI-minIP, and TOF-MRA were acquired. For the draining veins of the AVM identified on angiography, we analyzed signal intensity on the images listed above, and classified it into hyperintensity (hyper), mixed intensity (mixed), hypointensity (hypo) and no visualization.

Results: On the analysis of 27 angiographically proven draining veins, 19 draining veins were classified as hyper, 3 as mixed, 0 as hypo, and 6 as no visualization on SWI-mag. On TOF images, 21 draining veins were classified as hyper, 2 as mixed, 0 as hypo, and 4 as no visualization. While 6 draining veins did not show hyperintensity on TOF, SWI-mag visualized 3 of these 6 veins as hyper.

Conclusion: SWI-mag depicted most draining veins of AVM as hyperintensity. We speculate that this is mainly due to the higher concentration of oxy-Hb and in-flow effect of the draining vein. SWI-mag seems to be useful in analysis and follow up for

AVM as the signal on the image may reflect physiological status.

Keywords

Susceptibility weighted image, Magnitude image, arteriovenous malformation,

Magnetic resonance imaging

Introduction

Diagnosis of cerebral arteriovenous malformation has become less invasive due to advances in CT and MRI technologies. These modalities provide important information that can be used for treatment planning such as surgical resection, interventional procedures, radiation, and/or their combination. In addition to providing morphological information about the size, shape, and location of AVM, hemodynamic information including recognition of inflow arteries and outflow veins and flow speed are important for treatment planning [1, 2]. Digital subtraction angiography (DSA) is the gold standard for evaluating hemodynamic information. Magnetic resonance digital subtraction angiography (MR-DSA) is one option for evaluating hemodynamics of AVM. However, the spatial resolution is not sufficient for strict clinical use. Although CT angiography can provide good morphological and spatial information, temporal resolution is restricted due to radiation exposure.

SWI, which uses a fully flow compensated, long echo, gradient echo scan to acquire images, can identify susceptibility differences between tissues [3-5]. On SWI sequences, images are constructed from magnitude images (SWI-mag), which have a high resolution and long TE gradient echo image with flow compensation, and phase image, in which a high-pass filter is applied and used for making the phase mask. A phase mask

processed from the phase image is applied to the magnitude image, and finally, minimum intensity projection is applied to emphasize low signal structures such as cerebral veins.

In general, the draining vein of an AVM contains a larger amount of Oxy-Hb compared with a normal vein and is referred to as a “red vein” [6]. Theoretically, because draining veins of AVM have less susceptibility and higher flow speed, these veins are expected to show a high signal, such as arteries on SWI-mag. Although one report mentioned a high signal at the draining vein of AVM, no report has compared SWI-mag with DSA [7].

The purpose of this study is to evaluate signal characteristics of SWI for AVM, including original unprocessed magnitude images, especially for visualization of draining veins. For this purpose, we identified the feeding artery, nidus, and draining veins of AVM patients by using DSA and evaluated the signal characteristics of SWI-mag and SWI-minIP. We also evaluated the source image of time of flight magnetic resonance angiography (TOF MRA).

Materials and Methods

This retrospective study consists of consecutive patients in which MRI examination including SWI and DSA were performed from January 2006 to March 2011 in our

institute. Written informed consent for the imaging study, including DSA, was obtained from all patients after the nature of the procedure was fully explained. Subjects consisted of 14 patients with angiographically proven AVM (9 males, 5 females; mean age, 47.6 years; range, 19–67 years). Symptoms included hemorrhage (8 patients), seizure (2 patients), hemianopsia (1 patient), headache (1 patient), and 2 asymptomatic patients. The sizes of the AVM were less than 3 cm in 12 patients and 3 to 6 cm in 2 patients. Spetzler-Martin grades were 1 point in 4 patients, 2 points in 5 patients, 3 points in 4 patients, and 4 points in 1 patient. These patients were treated by embolization using an interventional procedure in 1 patient, a combination of embolization and surgical resection in 2 patients, a surgical procedure in 5 patients, and radiation therapy in 2 patients. Four patients were not treated and course watching was selected. The interval of MR imaging and DSA was within one month with the exception of two patients. In one of them the interval was 10 months and in the other the interval was 6 months.

DSA was performed on bi-plane equipment (Digitex-2400, Shimadzu Medical System, Kyoto, Japan). Using the Seldinger technique from the common femoral artery, a 5 French diameter catheter was selectively positioned in the internal carotid artery or vertebral artery. Then, selective angiographies were acquired using 6 ml of contrast

agent (Iopamiron 300, Schering AG, Germany) at a rate of 4 ml/sec. Images were obtained with 1024 x 1024 matrix and 2.5 frames/sec.

MR images were acquired using a 1.5T clinical scanner (Magnetom Avanto, Siemens AG, Erlangen, Germany) and the protocol included the following sequences: (1) SWI (velocity compensated gradient echo sequence TR=49 ms, TE=40 ms, FOV=256 mm, imaging matrix=256 x 256, slice thickness=1.6 mm); and (2) TOF image (flash sequence TR= 34-36 ms, TE=7.15ms, FA=25, FOV=20cm, matrix=320x320, slice thickness=0.65 mm). In addition of SWI and TOF-MRA, our protocol included axial image of T1 weighed imaging and T2 weighed imaging, sagittal image of T1 weighed imaging, coronal image of T2 weighed imaging and diffusion weighted imaging.

SWI-minIP was obtained automatically on console at MR suite to create minimum intensity projections over 12.8 mm. Image observations were made using a picture archiving and communication system viewer. SWI images including SWI-mag, SWI-minIP, and original images of TOF-MRA were observed.

First, we identified the feeding arteries, nidus, and draining veins of the AVM by analyzing the early arterial to late venous phases of DSA images. For items identified on DSA, we analyzed the following points: (1) signal on SWI-mag, (2) signal on SWI-minIP, and (3) signal on TOF image. Signals on these images were evaluated

visually by the consensus of 2 neuroradiologists (TM, TT) as hyperintensity to white matter (hyper), mixed intensity (mixed), hypointensity to the white matter (hypo), or no visualization. Mixed intensity was defined as having both hyperintensity and hypointensity.

In addition we analyzed patients in which the draining vein did not show hyperintensity on TOF images and looked at the signal of the draining vein on SWI images.

Results

Findings on DSA images showed that the location of AVM was frontal in 4 patients, parietal in 2 patients, occipital in 2 patients, temporal in 1 patient, in the thalamus in 1 patient, in the lateral wall of the ventricle in 1 patient, and in the posterior fossa in 3 patients. Twenty-one feeding arteries were identified in total, with up to 5 arteries in 1 patient. Twenty-seven draining veins were identified in total, with up to 4 draining veins in 1 patient (Figures 1 to 3).

For the analysis of feeding arteries, 17 of 21 arteries were classified as hyper (81.0%), 1 as mixed (4.8%), 2 as hypo (9.5%), and 1 as no visualization (4.8%) on SWI-mag. On SWI-minIP, no arteries were classified as hyper or mixed, 13 were classified as hypo (61.9%), and 8 were classified as no visualization (38.1%). On TOF images, 21 feeding

arteries were classified as hyper (100%) and none showed hypo, mixed, or no visualization (Figure 4A).

The signal of the nidus was also analyzed on SWI-mag and 5 of 14 nidus were classified as hyper (35.7%), 8 as mixed (57.1%), 0 as hypo (0%), and 1 as no visualization (7.1%). On SWI-minIP, 1 nidus was classified as hyper (7.1%), 2 as mixed (14.3%), 7 as hypo (50.0%), and 4 as no visualization (28.6%). On TOF images, in patients for which TOF images were acquired, 14 nidus were classified as hyper (100%) and none showed hypo or no visualization (Figure 4b).

In the analysis of the signal of the draining vein, 19 of 27 draining veins were classified as hyper (70.4%), 2 as mixed (7.4%), 0 as hypo (0%), and 6 as no visualization (22.2%) on SWI-mag. On SWI-minIP, no draining vein was classified as hyper (0%), 0 as mixed (0%), 10 as hypo (37.0%), and 17 as no visualization (63.0%). On TOF images, 21 draining veins were classified as hyper (77.8%), 2 as mixed (7.4%), 0 as hypo (0%), and 4 as no visualization (14.8%) (Figure 4c).

There were 6 draining veins that did not show hyperintensity on TOF images including 2 mixed and 4 no visualization. The signal intensity of these 6 draining veins on SWI-mag was classified as hyper for 3 veins (50%), mixed for 1 vein (16.7%), hypo for 0 veins (0%), and no visualization for 2 veins (33.3%). On SWI-minIP, no draining vein

was classified as hyper (0%), 0 as mixed (0%), 2 as hypo (33.3%), and 4 as no visualization (66.7%) (Figure 4d).

Discussion

AVM are congenital vascular lesions that consist of direct connections between arteries and veins, without an intervening capillary bed. Estimates of the prevalence of brain AVMs in the general population range from 0.5 to 1.8 per 100,000 population per year [8, 9]. The incidence of first-ever AVM hemorrhage is 0.51 per 100,000 population per year [10]. Treatment for AVM includes surgical resection, embolization by interventional procedure, radiosurgery, or a combination of these methods [11, 12]. As interventional procedures and stereotactic radiosurgery methods have progressed, treatment strategies have been altered and some controversies have arisen [13]. Information about the status of the draining vein, degree of shunt flow, existence of an aneurysm or varix, and size and location of the nidus are important for treatment selection. It is also important to evaluate the hemodynamics of the lesion during follow up of patients [14]. DSA is still the gold standard for evaluation of AVM morphology and hemodynamics. However, the procedure is invasive and has some risk for side effects; thus, non- or less-invasive methods are desirable, especially for repeated follow

ups. CT angiography has shown great potential [15]. Morphological information can be readily depicted and spatial resolution is sufficient. However, due to the problem of radiation exposure, the time resolution is restricted; thus, it is difficult to evaluate hemodynamics by CT angiography. MRA is a powerful tool for evaluating arterial structures of the brain. Both the feeding artery and the nidus are clearly depicted by TOF-MRA, and this method provides morphological information with high spatial resolution [16]. However, depiction of the draining vein is insufficient, and it is difficult to obtain hemodynamic information. Although MR-DSA allows for evaluation of hemodynamics by MRI, spatial resolution is not sufficient [17].

In the current study, TOF images generally depicted feeding arteries, the nidus, and draining veins with high signals. SWI-mag showed high signals on feeding arteries and most of the draining veins. Some patients were judged as having a mixed intensity, in which the margin of the vessel showed a higher signal and the center of the vessel showed a lower signal, possibly due to a dephasing effect caused by the long TE of the sequence and high flow of the vein. SWI-minIP showed feeding arteries, the nidus, and draining veins as uniformly having a low signal, making discrimination between arterial and venous structures difficult. It is because of inherent for the minimal intensity projection. In general, the draining vein showed a higher signal by TOF than SWI-mag;

however, 6 veins did not show a high signal on TOF images and 3 of them were depicted as having a high signal on SWI-mag. For both the SWI-mag and TOF image, the existence of a hemorrhage was a major factor involved in the worsening visualization of these vessels.

SWI is an imaging technique that maximizes the sensitivity to susceptibility effects and has exquisite sensitivity to the venous vasculature, blood products, and changes in iron content. The sequence uses a gradient echo technique with post-processing that provides sensitive detection of paramagnetic effects by combining magnitude information and filtered phase information [3-5]. The SWI-mag is the source image of SWI, which is a 3D gradient echo sequence with a long TE, short TR, small flip angle, high resolution, and full velocity compensation. Thus, it is not a simple gradient echo T2* weighted image. Although it has a long TE, the small flip angle suppresses the signal from the cerebrospinal fluid and the short TR suppresses the signal from the brain parenchyma. The full velocity compensation prevents the signal within vessels from decreasing due to a dephasing effect from a long TE. Thus, the arteries show a high signal on SWI-mag. In contrast, TOF images consist of a sequence that emphasizes the arterial signal by the inflow effect by using a short TE and adjusting transverse magnetization via a ramped radiofrequency pulse. As a result, an arterial high signal on TOF images primarily

depends on the flow speed. At 1.5 T, depending on the concentration of deoxygenated-hemoglobin (deoxy Hb) and oxygenated-hemoglobin (oxy Hb), arterial blood has a T2* of about 200 msec, and venous blood (70% saturated) has a T2* of about 100 msec due to the susceptibility effect from deoxy Hb. On the SWI-mag, the high signal of the artery mainly depends on rephasing by velocity compensation gradients and high concentrations of oxy-Hb within the vessels that prevent the signal decrease via the susceptibility effect from deoxy-Hb. In the draining vein, the concentration of the oxy-Hb is higher than in normal veins and the flow speed is higher than in normal veins [18]. Thus, the draining vein shows high signal both on TOF image and the SWI-mag. In particular, when the flow speed of the draining vein is higher, the TOF images tends to depict the vein with a higher signal; however, when the flow speed of the draining vein is lower, the SWI-mag seems to have merit as it depicts the vein with a high signal. The Advantages and disadvantages of SWI-mag, SWI-minIP and TOF are summarized in table1.

SWI is useful to detect microbleeding [19]. However, on SWI-minIP, when there is microbleeding within the lesion, it is difficult to assess vascular anatomy, because microbleedings, the feeding artery, and the draining vein are described as having a low signal. In addition, SWI-minIP is sensitive to hemorrhagic products, so a blooming

effect may disturb observation of fine vessel structure. SWI-mag can be used as a complement to back up the resolution of the vascular anatomy without being severely disturbed by a strong susceptibility effect from microbleedings, as it is less sensitive to blooming. In addition, it brings unique information about oxygenation within the vein that can only be provided by this image. Theoretically, as mentioned above, the magnitude image can depict the draining vein better than the TOF image when the flow speed of the vein is slow. Although TOF can visualize a rather high-flow draining vein due to its pulse design, the information mainly depends on flow speed, which is different from that obtained on SWI-mag. In that sense, TOF images and SWI-mag provide very different information and can be complementary in nature. In particular, for patients with slow shunt flow patients such as patients after treatment by intravascular embolization, follow up examination by TOF is difficult and DSA may be necessary. Information by SWI-mag may not change the selection of treatment in the clinical practice, since DSA is still golden standard for evaluating morphology and hemodynamics of the AVMs. However, use of the SWI-mag can be useful in the follow up study after treatment. Although slow shunts were often visualized poorly on TOF-MRA, SWI-mag could demonstrate draining veins of slow-shunted AVM as hyperintensity. Red vein, which is visualized as high intensity on magnitude images, is

one of the good indicators of recurrence and progression.

The current study has some limitations, including a small number of patients. However, we could evaluate 24 draining veins from 11 patients, which covered various flow statuses. There were two patients in which interval of MR imaging and DSA was as long as 10 months and 6 months. Another limitation is that we used DSA as the gold standard and tried to evaluate the draining vein identified by DSA. As a result, the group of draining veins evaluated does not contain veins that were depicted only on MRI. In addition, our statement on the flow effects on SWI signal intensity is still speculative.

We could not delineate the impact of turbulent flow and pulsation artifacts of veins with an arterial flow pattern due to the AV-shunting.

We selected white matter as standard for comparison of the vessel signal in the current study, not the normal veins. One of the reasons of the selection is the difficulty in comparing signal intensity of the draining veins with the normal vein, since the signal of normal veins on SWI are not uniform. The other reason is that it is difficult to determine “normal” veins in AVM cases. In addition, the major reason for this selection is that the difference between the signal intensity of the draining veins and the surrounding structure is the most useful in pointing out the draining vein in the clinical practice.

In conclusion, magnitude images for SWI depict large number of draining veins of

AVM as hyperintensity, even when hyperintensity in draining veins cannot be visualized on TOF images. We speculate that this phenomenon is mainly due to the higher concentration of oxy-Hb and in-flow effect of the draining vein. Thus, the hyperintensity of draining veins of AVM on magnitude image of SWI may reflect the pathophysiology of AVM, and can be helpful in pre-treatment workup and post-treatment follow up, especially when the draining veins do not show hyperintensity on TOF image due to slow flow.

Conflict of interest: We declare that we have no conflict of interest.

References

1. Ogilvy CS, Stieg PE, Awad I, Brown RD, Jr., Kondziolka D, Rosenwasser R, Young WL, Hademenos G (2001) AHA Scientific Statement: Recommendations for the management of intracranial arteriovenous malformations: a statement for healthcare professionals from a special writing group of the Stroke Council, American Stroke Association. *Stroke* 32 (6):1458-1471
2. Yuki I, Kim RH, Duckwiler G, Jahan R, Tateshima S, Gonzalez N, Gorgulho A, Diaz JL, De Salles AA, Vinuela F (2010) Treatment of brain arteriovenous malformations with high-flow arteriovenous fistulas: risk and complications associated with endovascular embolization in multimodality treatment. Clinical article. *J Neurosurg* 113 (4):715-722. doi:10.3171/2009.9.JNS081588
3. Haacke EM, Xu Y, Cheng YC, Reichenbach JR (2004) Susceptibility weighted imaging (SWI). *Magn Reson Med* 52 (3):612-618. doi:10.1002/mrm.20198
4. Sehgal V, Delproposito Z, Haacke EM, Tong KA, Wycliffe N, Kido DK, Xu Y, Neelavalli J, Haddar D, Reichenbach JR (2005) Clinical applications of neuroimaging with susceptibility-weighted imaging. *J Magn Reson Imaging* 22 (4):439-450. doi:10.1002/jmri.20404
5. Haacke EM, Mittal S, Wu Z, Neelavalli J, Cheng YC (2009) Susceptibility-weighted

- imaging: technical aspects and clinical applications, part 1. *AJNR Am J Neuroradiol* 30 (1):19-30. doi:ajnr.A1400
6. Barnett GH, Little JR, Ebrahim ZY, Jones SC, Friel HT (1987) Cerebral circulation during arteriovenous malformation operation. *Neurosurgery* 20 (6):836-842
 7. George U, Jolappara M, Kesavadas C, Gupta AK (2010) Susceptibility-weighted imaging in the evaluation of brain arteriovenous malformations. *Neurol India* 58 (4):608-614. doi:ni_2010_58_4_608_68668
 8. Stapf C, Mast H, Sciacca RR, Berenstein A, Nelson PK, Gobin YP, Pile-Spellman J, Mohr JP (2003) The New York Islands AVM Study: design, study progress, and initial results. *Stroke* 34 (5):e29-33. doi:10.1161/01.STR.0000068784.36838.19
 9. Al-Shahi R, Bhattacharya JJ, Currie DG, Papanastassiou V, Ritchie V, Roberts RC, Sellar RJ, Warlow CP (2003) Prospective, population-based detection of intracranial vascular malformations in adults: the Scottish Intracranial Vascular Malformation Study (SIVMS). *Stroke* 34 (5):1163-1169. doi:10.1161/01.STR.0000069018.90456.C9
 10. Stapf C, Labovitz DL, Sciacca RR, Mast H, Mohr JP, Sacco RL (2002) Incidence of adult brain arteriovenous malformation hemorrhage in a prospective population-based stroke survey. *Cerebrovasc Dis* 13 (1):43-46. doi:ced13043
 11. Starke RM, Komotar RJ, Hwang BY, Fischer LE, Garrett MC, Otten ML, Connolly

- ES (2009) Treatment guidelines for cerebral arteriovenous malformation microsurgery. *Br J Neurosurg* 23 (4):376-386. doi:913449437
12. Soderman M, Andersson T, Karlsson B, Wallace MC, Edner G (2003) Management of patients with brain arteriovenous malformations. *Eur J Radiol* 46 (3):195-205. doi:S0720048X03000913
13. Starke RM, Komotar RJ, Hwang BY, Fischer LE, Otten ML, Merkow MB, Garrett MC, Isaacson SR, Connolly ES, Jr. (2008) A comprehensive review of radiosurgery for cerebral arteriovenous malformations: outcomes, predictive factors, and grading scales. *Stereotact Funct Neurosurg* 86 (3):191-199. doi:000126945
14. Geibprasert S, Pongpech S, Jiarakongmun P, Shroff MM, Armstrong DC, Krings T (2010) Radiologic assessment of brain arteriovenous malformations: what clinicians need to know. *Radiographics* 30 (2):483-501. doi:30/2/483
15. Gupta V, Chugh M, Walia BS, Vaishya S, Jha AN (2008) Use of CT angiography for anatomic localization of arteriovenous malformation Nidal components. *AJNR Am J Neuroradiol* 29 (10):1837-1840. doi:ajnr.A1136
16. Tanaka H, Numaguchi Y, Konno S, Shrier DA, Shibata DK, Patel U (1997) Initial experience with helical CT and 3D reconstruction in therapeutic planning of cerebral AVMs: comparison with 3D time-of-flight MRA and digital subtraction

angiography. *J Comput Assist Tomogr* 21 (5):811-817

17. Tsuchiya K, Katase S, Yoshino A, Hachiya J (2000) MR digital subtraction angiography of cerebral arteriovenous malformations. *AJNR Am J Neuroradiol* 21 (4):707-711
18. Divani AA, Lieber BB, Wakhloo AK, Gounis MJ, Hopkins LN (2001) Determination of blood flow velocity and transit time in cerebral arteriovenous malformation using microdroplet angiography. *Ann Biomed Eng* 29 (2):135-144
19. Iwamura A, Taoka T, Fukusumi A, Sakamoto M, Miyasaka T, Ochi T, Akashi T, Okuchi K, Kichikawa K (2011) Diffuse vascular injury: convergent-type hemorrhage in the supratentorial white matter on susceptibility-weighted image in cases of severe traumatic brain damage. *Neuroradiology*. doi:10.1007/s00234-011-0892-9

Table 1

The advantages and disadvantages of SWI-mag, SWI-minIP and TOF

Advantages

SWI-mag •Draining veins are visualized as hyperintensity.

SWI-minIP •Dilated veins are well depicted.

- A small amount of hemosiderin is emphasized.

TOF •The feeding arteries, nidus, draining veins are depicted in detail.

Disadvantages

SWI-mag •Discrimination of feeding arteries and draining veins are sometimes confusing.

SWI-minIP •Feeding arteries are not visualized clearly.

- A large hemorrhage shows severe blooming.

- Feeding arteries and draining veins are not discriminated.

TOF • Discrimination of feeding arteries and draining veins are sometimes confusing.

Figure 1

A 41-year-old female patient with hemorrhagic AVM of the left thalamus.

A, lateral view of the left vertebral angiography shows nidus and thick draining vein (arrow). B, TOF images show high signal intensity in the draining vein (arrow). C, the draining vein is not clearly demonstrated on SWI (arrow). D, magnitude images present high signal intensity in the draining vein (arrow).

Figure 2

A 39-year-old male with AVM in the right frontal AVM.

Initial symptom was convulsion. A, Right carotid angiography: Nidus in the frontal lobe and several draining veins are visualized. Right thalamostriate vein (arrow) is one of the draining veins. B, On the TOF image, there is no visualization of the right thalamostriate vein. C, T2 weighted images show low signal flow void image of the right thalamostriate vein. D, SWI-mag shows hyperintensity at the right thalamostriate vein.

Figure 3

A 53-year-old male patient with AVM in the left occipital lobe.

A, Venous phase of the left carotid angiography shows slow-flow AVM with 2 thick and serpentine draining veins. B, TOF images show high intensity in the superficial cerebral vein. C, Magnitude image shows mixed intensity. D, SWI shows hypointensity.

Figure 4

A, Visualization of the feeders on SWI and TOF images.

All feeding arteries showed hyperintensity on TOF images due to high flow speed. On SWI mag, 17 of 21 feeding arteries (81%) showed hyperintensity. The hyperintensity of the feeding artery on SWI-mag may be due to high flow and high oxygen concentration of the arteries.

B, Visualization of the nidus on SWI and TOF images.

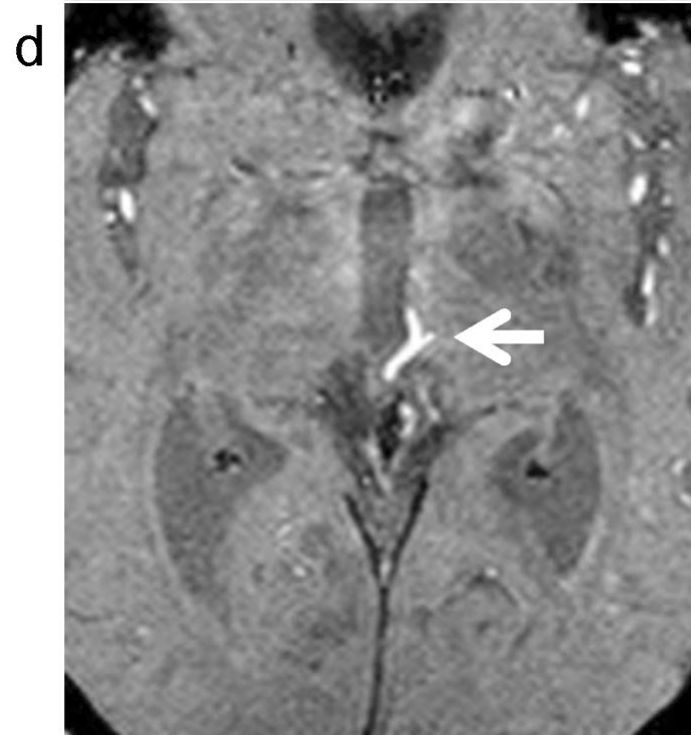
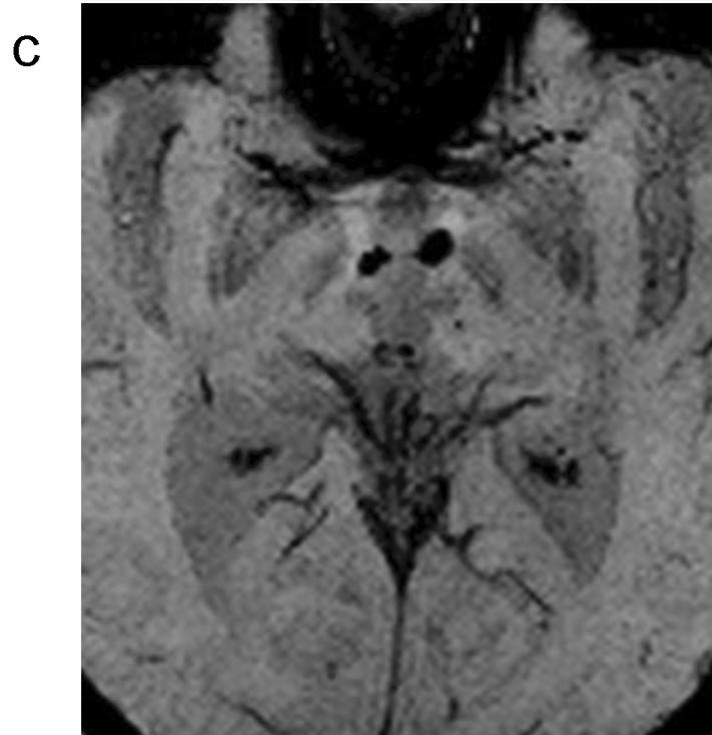
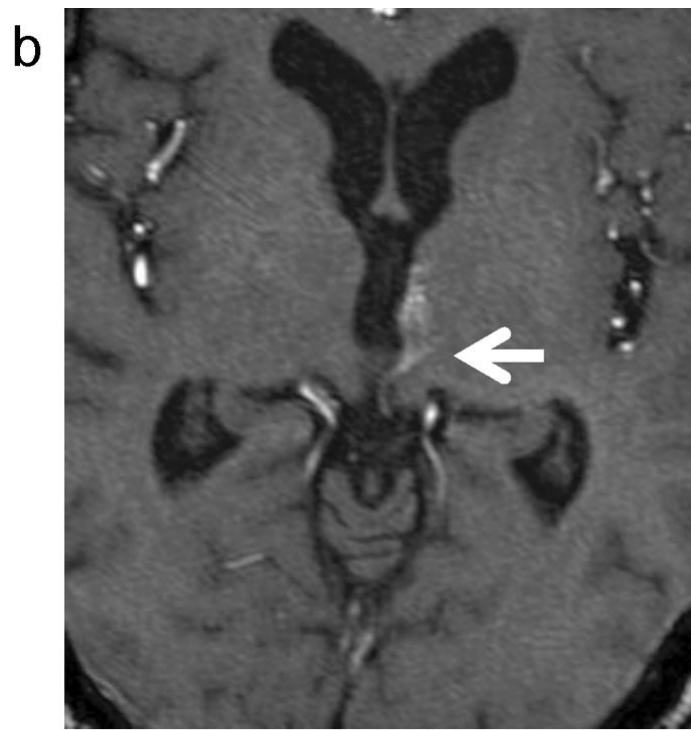
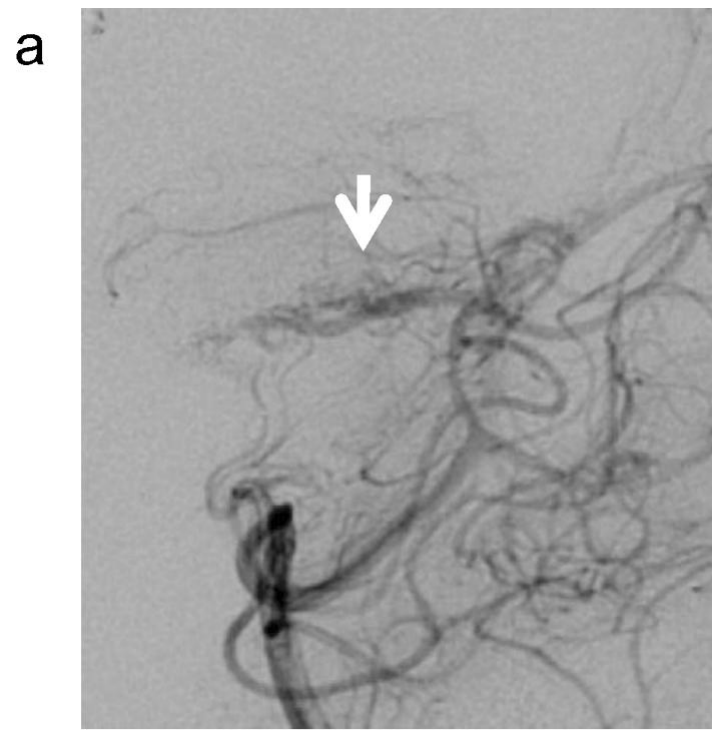
The nidus also showed hyperintensity on TOF images in all patients. In contrast, a small number of nidus showed hyperintensity on SWI-mag and SWI-minIP. These were due to signal decreases due to bleeding within the nidus in most patients.

C, Visualization of the draining veins on SWI and TOF images.

In contrast to the feeding artery and nidus, 6 of 27 draining veins (22.2%) did not showed hyperintensity on TOF images. On SWI-mag, 19 draining veins were classified as hyper (70.4%).

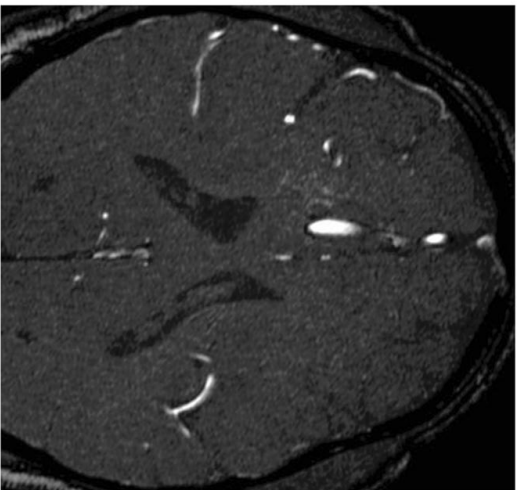
D, Signal intensity on SWI images of the draining veins which did not show hyperintensity on TOF image.

Among these 6 draining veins that did not showed hyperintensity on TOF in Figure 4C, SWI-mag showed hyperintensity for 3 veins (50%), mixed intensity for 1 vein (16.7%), hypointensity for 0 veins (0%), and no visualization for 2 veins (33.3%). When the flow speed of the draining vein is lower, the SWI-mag seems to have merit as it depicts the vein as hyperintensity while TOF does not depict the vein as hyperintensity.

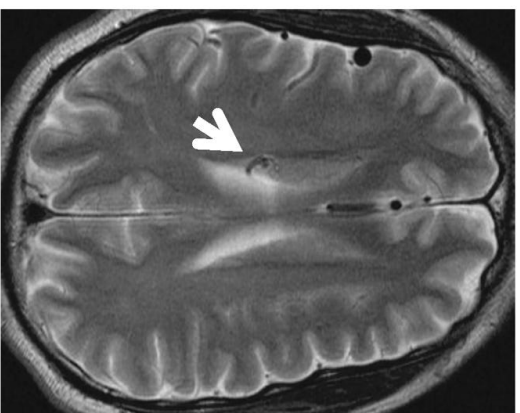




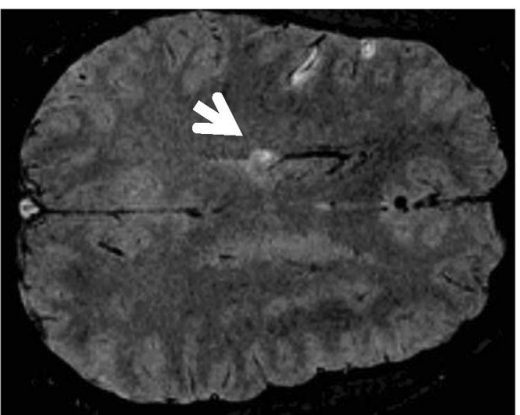
a



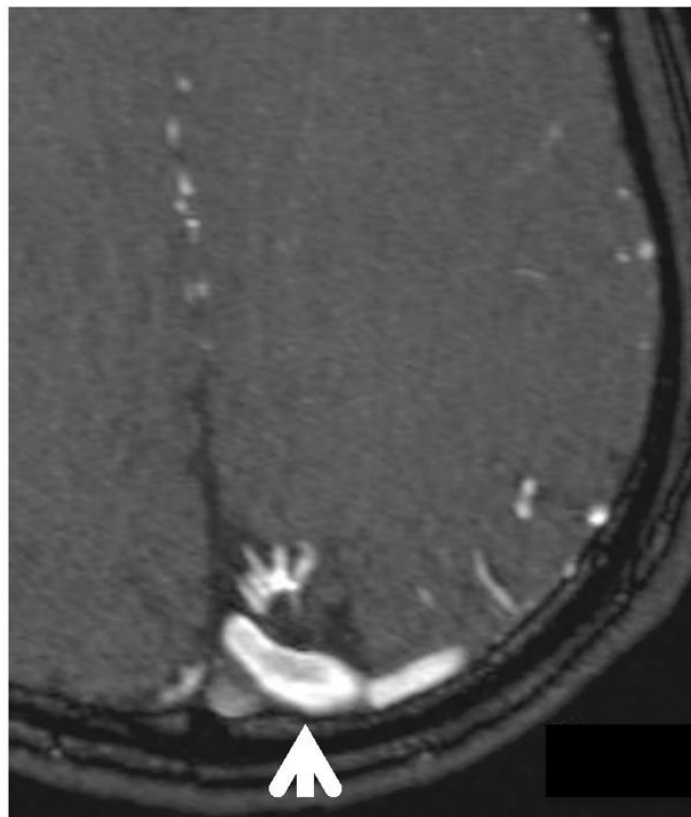
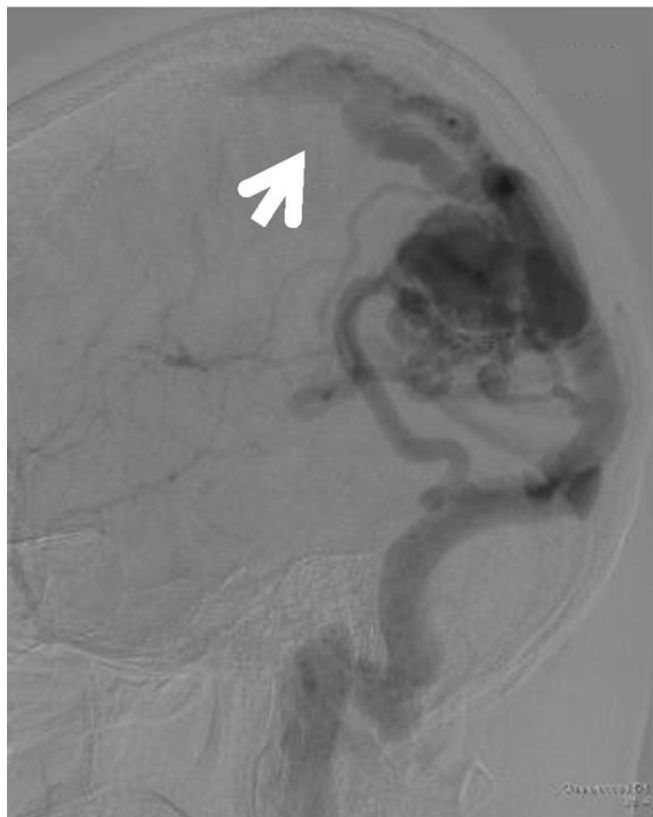
b



c

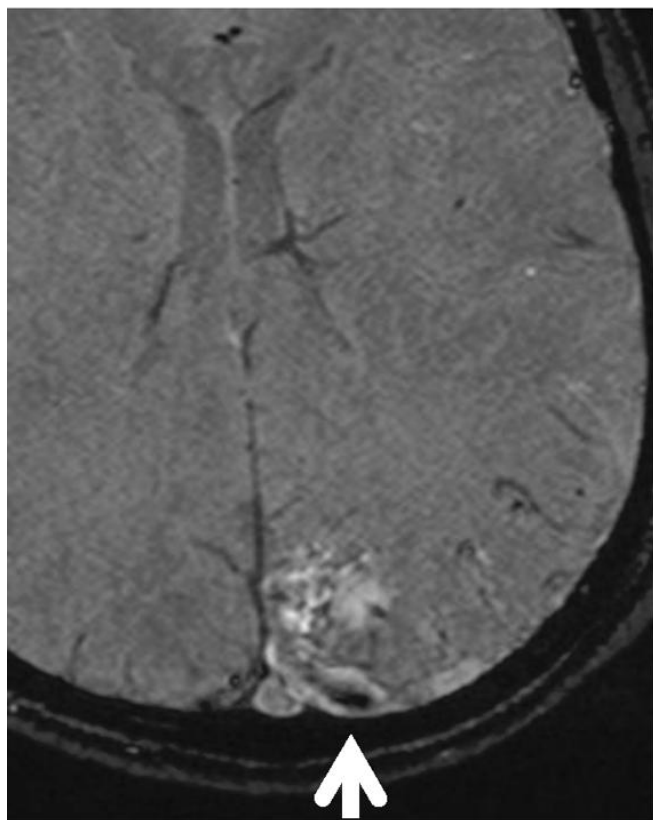


d

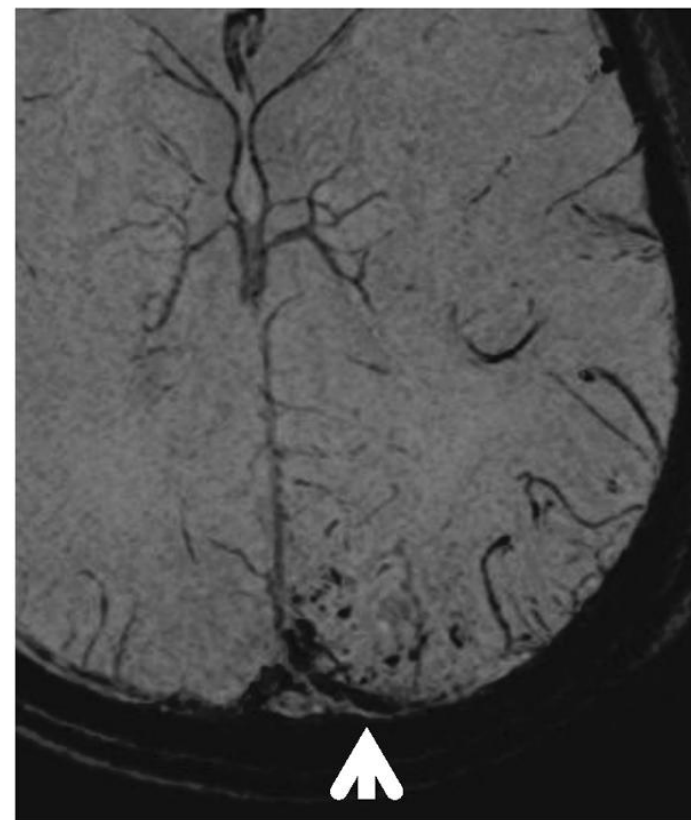


a

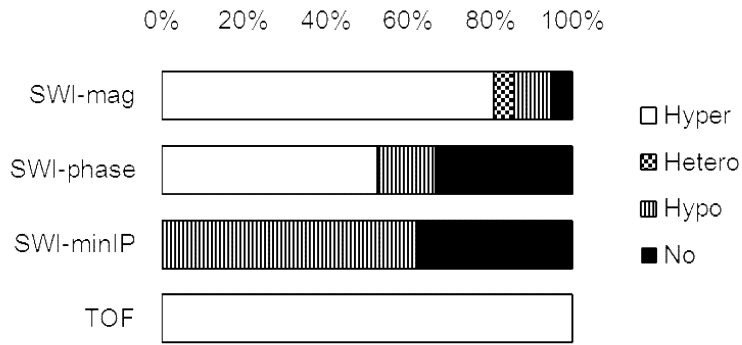
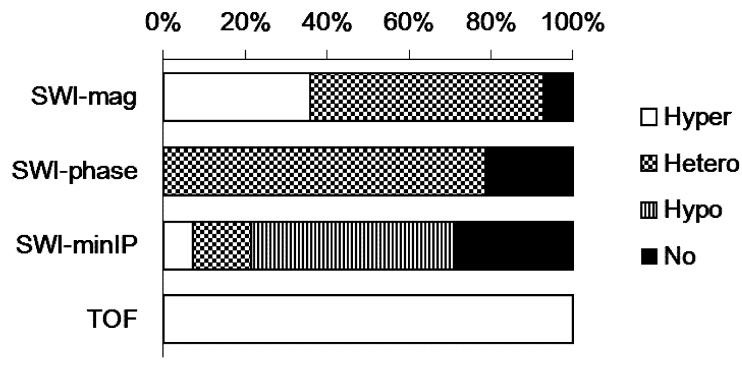
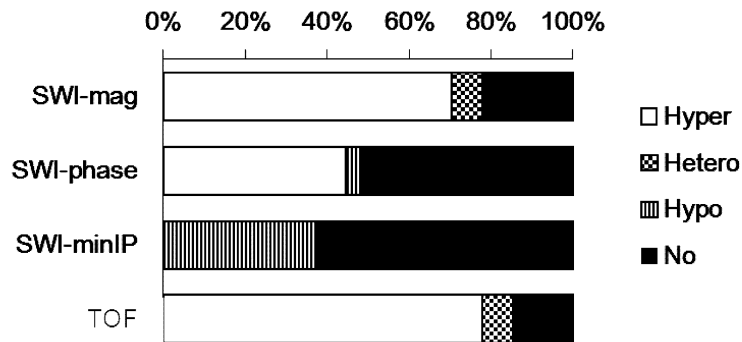
b



c



d

a**Feeding arteries****b****Nidus****c****Draining veins****d****Draining veins which did not show hyperintensity on TOF image**